Manuscript
Click here to download Manuscript: manuscript0707.doc

Title page

Title: Visual prognosis of eyes with submacular hemorrhage associated with exudative age-related macular degeneration

Running title: Submacular hemorrhage from AMD

Authors: Naoko Ueda-Arakawa, MD, Akitaka Tsujikawa, MD, Kenji Yamashiro, MD, Sotaro Ooto, MD, Hiroshi Tamura, MD, Nagahisa Yoshimura MD

Institutions: Department of Ophthalmology and Visual Sciences, Kyoto University Graduate School of Medicine, Kyoto, Japan.

Correspondence to: Akitaka Tsujikawa, Department of Ophthalmology and Visual Sciences, Kyoto University Graduate School of Medicine, 54 Shogoin-Kawahara-cho, Sakyo-ku, Kyoto 606-8507, Japan.

fax: +81-75-752-0933; tel: +81-75-751-3260; e-mail: tujikawa@kuhp.kyoto-u.ac.jp

Word counts for the abstract, 200; the main text, 3271.

The number of references, 43; number of figures, 4; number of tables, 4.

Abstract

Purpose To study the retinal structural changes associated with submacular hemorrhage due to exudative age-related macular degeneration (AMD) and their relationships with visual prognosis.

Methods We retrospectively reviewed the medical records of 31 consecutive patients (31 eyes) with visual impairment due to an acute submacular hemorrhage associated with typical AMD (10 eyes) or polypoidal choroidal vasculopathy (21 eyes).

Results Optical coherence tomography (OCT) revealed that submacular hemorrhages exhibited intense hyperreflectivity beneath the neurosensory retina and often seemed to infiltrate the overlying neurosensory retina. In OCT sections, mild to moderate amorphous hyperreflectivity and/or hyperreflective dots were observed within the neurosensory retina, resulting in the lack of the junction between the inner and outer segments of the photoreceptors (IS/OS). Of the 31 eyes, the foveal IS/OS line could be seen incompletely in 12 eyes and absent in 16 eyes. The initial integrity of the foveal photoreceptor layer was correlated with final visual acuity; the initial detection of the IS/OS just beneath the fovea was correlated with good final visual acuity ($r = 0.375$, $p = 0.038$).

Conclusion As a hallmark of integrity of the foveal photoreceptor layer, the initial detection of the IS/OS just beneath the fovea may predict good visual outcomes.

Keywords Age-related macular degeneration; Optical coherence tomography; Polypoidal choroidal vasculopathy; Submacular hemorrhage.

Introduction

Submacular hemorrhage is just one of the many vision-threatening complications associated with exudative age-related macular degeneration (AMD) [1]. It can cause a sudden loss of central vision, often resulting in permanent visual loss [2]. The natural visual prognosis of submacular hemorrhage is extremely poor [3-6]. In a previous retrospective study by Bennett et al. [3], the mean initial visual acuity (VA) in eyes with submacular hemorrhage (20/860) improved to no better than 20/480 after a mean follow-up of 3 years. Numerous surgical procedures and several modifications have been described aimed at improving the poor visual prognosis [3-14]. For acute large submacular hemorrhage, surgical drainage or pneumatic displacement with or without tissue plasminogen activator is thought to improve the visual prognosis [8, 11-14]. However, the effectiveness of subretinal clot removal is limited [7, 8].

The exact mechanism remains unclear as to why a thick submacular hemorrhage can cause sudden visual loss, even when the sensory retina within the macular area is seen clearly on fundus examination [2]. Histologic reports have shown that submacular hemorrhage can cause substantial damage to the outer retina [16, 17]. In experimental studies with an animal model, Glatt and Machemer [18] have reported that the photoreceptors overlying areas of the hemorrhage appear to have degenerated and exhibit pyknosis within 24 hours. Subsequent reports have suggested other

mechanisms of damage to the photoreceptor layer, including clot retraction [19], iron toxicity [20, 21], and blockage of nutrient diffusion [2].

Optical coherence tomography (OCT) enables the detection of changes in the retinal architecture and quantitative measurement of retinal thickness [22-25]. Recent technologic advances in OCT have contributed to a more detailed understanding of the pathomorphology of many macular diseases [26-28]. However, there is still little information available on morphologic changes in the neurosensory retina associated with the submacular hemorrhage [15]. In addition, various factors are thought to be associated with visual prognosis in eyes with a submacular hemorrhage, including hemorrhage size [4, 6], elevation of the overlying retina [3, 4, 6], and etiology of the original disease [3, 5]. However, quantitative evaluations are limited. In the study described herein, we studied OCT sections of eyes with submacular hemorrhage associated with exudative AMD. This was done to elucidate the structural changes in the overlying neurosensory retina to measure each characteristic manifestation quantitatively and to study the associations between the structural changes and visual function. Based on the results of these evaluations, we can now prognosticate the visual outcome of eyes with acute submacular hemorrhage.

Subjects and Methods

For this observational case study, we retrospectively reviewed the medical records of 31 consecutive patients (31 eyes) with visual impairment due to an acute thick submacular hemorrhage associated with exudative AMD; each of these patients had visited the Macula Service of the Department of Ophthalmology at Kyoto University Hospital between April 2007 and March 2010. Of the 31 eyes, 10 had typical AMD and 21 had polypoidal choroidal vasculopathy (PCV). All 31 eyes included in this study exhibited a submacular hemorrhage just beneath the center of the fovea. Eyes with either a small subretinal hemorrhage with less than 1 disc area or an old yellowish discolored submacular hemorrhage were excluded. Each patient underwent angiography with a confocal laser scanning system (HRA-2, Heidelberg Engineering, Heidelberg, Germany). In the current study, the presence of choroidal neovascularization (CNV) was confirmed with fluorescein and indocyanine green angiography, which were performed either at the initial visit or after the resolution of the submacular hemorrhage. The diagnosis of PCV was based on indocyanine green angiography, which shows a branching vascular network that terminates in polypoidal swelling. Eyes with other macular abnormalities (e.g., pathologic myopia, idiopathic CNV, presumed ocular histoplasmosis, angioid streaks, other secondary CNV, or retinal arterial macroaneurysm) were excluded. Of the 31 eyes of our patients, 21 were treated with intravitreal injections of anti-vascular endothelial growth factor agents, 2 by

photodynamic therapy, and 1 by pneumatic displacement of the submacular hemorrhage. This study was approved by the Institutional Review Board of the Kyoto University Graduate School of Medicine and adhered to the tenets of the Declaration of Helsinki.

At the initial examination after the submacular hemorrhage occurred, each patient underwent a comprehensive ophthalmologic examination, including measurement of best-corrected VA, determination of intraocular pressure, indirect ophthalmoscopy, slit-lamp biomicroscopy with a non-contact lens, and examinations with the Spectralis HRA+OCT (Heidelberg Engineering). Using these initial OCT images, we measured the thickness of the neurosensory retina, thickness of the submacular hemorrhage, and the total foveal thickness (Fig. 1). When the retinal pigment epithelium (RPE) was not visible under the fovea because of an overlying thick submacular hemorrhage, the OCT measurements were made from the presumed RPE line obtained from a clearly detectable RPE line in a more peripheral retinal area not covered by the hemorrhage. Furthermore, to assess the integrity of the outer foveal photoreceptor layer, we examined the junction between the inner and outer segments of the photoreceptor (IS/OS) line and the external limiting membrane (ELM) line in the fovea. The statuses of the IS/OS and ELM lines under the fovea were defined as complete, incomplete, or absent. To assess the density of the submacular hemorrhage, the detection of the underlying RPE line was

also determined to be complete, incomplete, or absent.

At the final examination, all eyes showed complete resolution of the submacular hemorrhage beneath the fovea. At this examination, best-corrected VA was measured and indirect ophthalmoscopy, slit-lamp biomicroscopy with a non-contact lens, and examinations with the Spectralis HRA+OCT were performed. After the submacular hemorrhage was resolved, the patients often exhibited a subfoveal mass, which appeared as subretinal deposit or fibrosis on the fundus photograph. Since it was often difficult to determine its border with respect to the RPE, we performed 3 measurements in the fovea by using OCT images obtained at the final examination, including the thickness of the neurosensory retina, thickness of the subretinal mass and Bruch's membrane, and the total thickness (Fig. 1). The thickness of the neurosensory retina was defined as the distance between the vitreoretinal interface and the inner border of hyperreflectivity of either the RPE or the subretinal mass. The thickness of the subretinal mass and Bruch's membrane was defined as the distance between the outer border of the neurosensory retina and the fine straight line of the elastic fiber layer of the Bruch's membrane. Total thickness was defined as the distance between the vitreoretinal interface and the elastic fiber layer of Bruch's membrane. These measurements and evaluations were performed by one retinal specialist.

All statistical analyses were performed using StatView version 4.5 (SAS Institute,

Cary, NC, USA). All values are expressed as mean ± standard deviation. For statistical analysis, VA measured using a Landolt chart was converted to a logarithm of the minimal angle of resolution (logMAR). In the current study, 1 optic disc area is equal to 2.54 mm^2 based on an optic disc diameter of 1.8 mm [29]. Bivariate relationships were analyzed using Pearson's correlation coefficient. *P* values less than 0.05 were considered statistically significant.

Results

In the current study, 31 eyes of 31 patients (21 men and 10 women; age range, 66–93 years; mean age, 76.8 ± 7.4 years) with submacular hemorrhage were examined. Of the 31 eyes, 21 had PCV and 10 had typical AMD. Table 1 shows the characteristics of patients included in this study. The mean initial VA (logMAR) was 0.69 ± 0.45. The mean initial area and thickness of the submacular hemorrhage were 6.0 ± 3.1 disc areas and 315.0 ± 222.5 μm, respectively. The follow-up period was 11.3 ± 7.0 months, ranging from 3 to 28 months.

At the initial examination, each eye exhibited a submacular hemorrhage that affected the fovea. Upon OCT examination, the submacular hemorrhage exhibited intensive or moderate hyperreflectivity depending on its density beneath the neurosensory retina. Of the 31 eyes, the underlying RPE could not be seen at all in 8

because of the shadow cast by the submacular hemorrhage. In addition, the submacular hemorrhage from the CNV or polypoidal lesions seemed to infiltrate the overlying neurosensory retina in many cases. On OCT sections, mild to moderate amorphous hyperreflectivity and/or hyperreflective dots were seen in the overlying neurosensory retina, especially in the outer aspect, resulting in a lack of IS/OS or ELM lines (Fig. 2). Of the 31 eyes, the foveal IS/OS line could not be observed completely in 28, whereas the foveal ELM line could be observed completely in 21. Intraretinal hyperreflective lesions due to submacular hemorrhage were occasionally observed mainly outside the ELM. In these eyes, the ELM seemed to work as a blocking agent against the hemorrhage (Fig. 2).

Table 2 shows the relationships between initial VA and other measured values obtained at the initial examination. The etiology of the original disease (typical AMD or PCV) was not correlated with the initial VA (r = 0.194, $p = 0.300$). However, the size and thickness of the submacular hemorrhage were both correlated with initial VA (r = 0.411, $p = 0.022$; r = 0.485, $p = 0.0057$). In addition, detection of the RPE beneath the fovea, which seemed to reflect the density of the submacular hemorrhage, was correlated with initial VA (r = 0.479, $p = 0.0064$). While the thickness of the neurosensory retina was not correlated with initial VA (r = 0.203, $p = 0.274$), detection of the foveal ELM was correlated with initial VA (r = 0.423, $p = 0.018$).

At the final examination, all eyes exhibited complete absorption of the submacular hemorrhage, and the mean final VA was 0.69 ± 0.47 (logMAR). Cystoid macular edema was observed in 11 eyes. Twenty eyes exhibited a subretinal mass, the mean thickness of which, including the Bruch's membrane, was 169.5 ± 150.4 μm. In addition, submacular hemorrhages caused substantial damage to the overlying outer retina. The IS/OS and ELM lines were completely detected in only 3 and 16 eyes, respectively.

Table 3 shows the relationships between final VA and other measured values obtained at the final examination. The etiology of the original disease (typical AMD or PCV) was not correlated with the final VA (r = 0.249, p = 0.176). However, cystoid macular edema and subfoveal mass were correlated with poor final VA (r = 0.355, p = 0.050; r = 0.477, p = 0.0067). The total retinal thickness and the thickness of the subfoveal mass at the final examination were correlated with poor final VA (r = 0.607, p = 0.0003; r = 0.489, p = 0.0052). In addition, the integrity of the foveal photoreceptor layer contributed to foveal function. Detection of the IS/OS and ELM lines beneath the fovea were both strongly correlated with good final VA (r = 0.574, p = 0.0007; r = 0.756, p < 0.0001).

Table 4 shows the relationships between final VA and measured values obtained at the initial examination. The final VA was 0.86 ± 0.39 with typical AMD and 0.61 ± 0.49 with PCV (p = 0.176). The etiology of the original disease was not correlated with final

VA (r = 0.249, *p* = 0.176). Although submacular hemorrhage thickness and density were weakly correlated with final VA (r = 0.258, *p* = 0.161; r = 0.281, *p* = 0.126), the size of the submacular hemorrhage was not (r = 0.111, *p* = 0.554). However, the initial integrity of the foveal photoreceptor layer was correlated with visual prognosis. While the initial detection of the ELM beneath the fovea was not correlated with final VA (r = 0.063, *p* = 0.736), the initial detection of the IS/OS beneath the fovea was correlated with good final VA (r = 0.375, *p* = 0.038) (Figs. 3 and 4). In the subgroup analysis, eyes with typical AMD and PCV exhibited a similar tendency, respectively, although the correlations were not statistically significant (r = 0.566, *p* = 0.088 with AMD; r = 0.331, *p* = 0.142 with PCV); this is possibly due to the small number of eyes in each group.

Discussion

Acute serous retinal detachment associated with central serous chorioretinopathy does not usually cause a severe decrease in VA even if there is subretinal fluid under the fovea [30]. However, submacular hemorrhage often accompanies acute severe visual loss immediately after onset [2]. Histologic reports have shown that submacular hemorrhage causes severe damage to the outer retina [16, 17], and experimental reports have suggested mechanisms by which chronic damage to the photoreceptor layer occurs [18, 19]. However, in addition to chronic effects, bleeding within the

subretinal space can exert immediate effects on the neurosensory retina, thereby causing acute visual dysfunction [15].

The initial OCT sections of our patients revealed that the submacular hemorrhage exhibited hyperreflectivity beneath the neurosensory retina. In addition, the overlying neurosensory retina often exhibited hyperreflective lesions. In the current study, amorphous hyperreflectivity of various intensities and hyperreflective dots were observed in the outer aspect of the overlying neurosensory retina. Immediately after bleeding within the subretinal space, erythrocytes, macrophages, and fibrin can migrate easily into the outer retina and may destroy the integrity of the photoreceptor layer [31]. In eyes with PCV, Ooto et al. [32] recently reported the relationship between VA and fibrin infiltration within the neurosensory retina. In addition, Coscas et al. [27] have stated that bright hyperreflective spots and hyperreflective materials within the neurosensory retina could be derived from an inflammatory reaction and they indicate the activity of exudative AMD. Based on previous reports [32, 33], our findings related to the neurosensory retina may be associated with acute dysfunction of the macula, which results in an acute loss of central vision.

In the current study, while the IS/OS line beneath the fovea was detected completely at the initial visit in only 3 eyes, complete detection of the ELM line under the fovea was achieved in 21 eyes. In fact, the ELM line frequently was preserved even in

the eyes with a thick submacular hemorrhage. On OCT sections, the ELM line sometimes appeared to act as a blocking agent against the advancement of hemorrhage into the retina after the hemorrhage had already infiltrated the inner and outer segments. Our OCT findings can be explained according to the theory on the mechanisms of fluid movement proposed by Marmor [34]. He reports that the ELM, which consists of the zonular adherens between Müller cells and photoreceptors at the base of the outer segments, works as a weak anatomic barrier to the movement of large protein molecules in the retina.

Previous reports on the natural history of submacular hemorrhage suggest that exudative AMD is associated with poor visual prognosis especially when subretinal fibrosis is observed after the resolution of the hemorrhage [3, 5]. In the current study, 64.5% of the eyes exhibited a subfoveal mass at the final examination; the thickness of this mass was strongly correlated with final VA. In addition, recent studies with OCT show that the integrity of the foveal photoreceptor layer—especially its outer aspect—is necessary if good visual function is to be achieved [35]. A few years ago, Hayashi et al. [36] reported the association between intact foveal IS/OS and good VA after the successful treatment of exudative AMD with photodynamic therapy. More recently, Oishi et al. [37] suggested that foveal ELM is associated with final VA in exudative AMD treated with photodynamic therapy. Consistent with these reports [36, 37], our study

shows that after complete resolution of the submacular hemorrhage, complete detection of the IS/OS and ELM lines are correlated with final VA.

So far, various factors are suggested to be associated with visual prognosis, including the initial VA [4, 5], size or thickness of the submacular hemorrhage [3, 4, 6], and etiology of the original disease [3, 5]. As mentioned above, visual prognosis was poor in eyes with submacular hemorrhage resulting from exudative AMD [3], especially in eyes with subretinal CNV [5]. While the relationship between the size of the hemorrhage and final VA varies, most previous studies indicate that the initial thickness of the hemorrhage is associated with visual prognosis [3, 4, 6]. However, in those studies, the thickness of the submacular hemorrhage was evaluated as elevation of the neurosensory retina detected by stereoscopic photography; no quantitative evaluations were performed. In the current study, the initial size of the hemorrhage was not correlated with final VA. However, the thickness and density of the hemorrhage were both weakly correlated with final VA.

It is a certainty that the integrity of the outer photoreceptor layer in the fovea contributes to VA [35-38]. In the current study, initial detection of the ELM line beneath the fovea was correlated with initial but not final VA. While the foveal ELM was initially detected in 21 eyes, complete detection was achieved at the final examination in only 16 eyes. The chronic harmful effects of submacular hemorrhage include damage to the

foveal photoreceptor layer, which results in a decline in VA [16]. However, the initial detection of the foveal IS/OS line was correlated with visual prognosis. The inner and outer segments of the photoreceptor layer located outside the ELM, which are assumed to function as a blockade against hemorrhage infiltration [34], are vulnerable to acute submacular hemorrhage [19, 39]. The foveal IS/OS line was detected completely at the initial visit in only 3 of our patients. In such eyes, acute effects on the neurosensory retina may be minimal, resulting in good visual prognosis.

In experimental studies with animal models, the suggested mechanisms of damage to the photoreceptor layer include clot retraction [19], iron toxicity [20, 21], and blockage of nutrient diffusion by iron [18]. Submacular hemorrhage may block the exchange of nutrients and metabolites between the neurosensory retina and RPE [18]. The chief toxic agent released from submacular hemorrhage is thought to be iron in the form of ferritin [2]. In an experimental model of submacular hemorrhage, increased iron levels in the outer segments of the photoreceptor layer are thought to exert a toxic effect to outer segment lipids via oxidative stress [39]. In addition, a previous experimental study by Toth et al. [19] showed that fibrin produced by submacular hemorrhage interdigitates with outer photoreceptor segments and subsequently tears the sheet of inner and outer photoreceptor segments. In the current study, the detection of the foveal IS/OS line at the initial examination was correlated with good final VA. In these

eyes, the lack of fibrin interdigitation and the low level of iron toxicity could explain the good visual prognosis.

The limitations of the current study include its retrospective nature, various treatment regimen used, and small sample size. Treatment modality may have some influence on the visual prognosis [40, 41]. Several factors may be mutually related ,but the number of eyes was too small to perform multiple univariate testing. In addition, while no eyes showed residual submacular hemorrhage at the final visits, follow-up period of some eyes were too short to discuss on the visual prognosis [42]. Another limitation is that the current study involved eyes with typical AMD and PCV. However, despite these limitations, our findings suggest that submacular hemorrhages often infiltrate the overlying neurosensory retina, harming the structure of the outer retina. As a hallmark of the integrity of the foveal photoreceptor layer, the initial detection of the IS/OS just beneath the fovea may be associated with good visual outcomes. Previous studies report a better visual prognosis for PCV [43]. We analyzed the subgroups of typical AMD and PCV to confirm the correlation between the initial detection of the foveal IS/OS and final VA. Each group exhibited a similar tendency, but the correlation was not statistically significant possibly because of the small number of eyes in each group. Further prospective studies are necessary to confirm the correlations reported in the current study.

References

1. Woo JJ, Lou PL, Ryan EA, Kroll AJ. Surgical treatment of submacular hemorrhage in age-related macular degeneration. Int Ophthalmol Clin. 2004;44:43-50.
2. Steel DH, Sandhu SS. Submacular haemorrhages associated with neovascular age-related macular degeneration. Br J Ophthalmol. 2011;95:1051-7.
3. Bennett SR, Folk JC, Blodi CF, Klugman M. Factors prognostic of visual outcome in patients with subretinal hemorrhage. Am J Ophthalmol. 1990;109:33-7.
4. Avery RL, Fekrat S, Hawkins BS, Bressler NM. Natural history of subfoveal subretinal hemorrhage in age-related macular degeneration. Retina. 1996;16:183-9.
5. Berrocal MH, Lewis ML, Flynn HW Jr. Variations in the clinical course of submacular hemorrhage. Am J Ophthalmol. 1996;122:486-93.
6. Scupola A, Coscas G, Soubrane G, Balestrazzi E. Natural history of macular subretinal hemorrhage in age-related macular degeneration. Ophthalmologica. 1999;213:97-102.
7. de Juan E Jr, Machemer R. Vitreous surgery for hemorrhagic and fibrous complications of age-related macular degeneration. Am J Ophthalmol. 1988;105:25-9.
8. Wade EC, Flynn HW Jr, Olsen KR, Blumenkranz MS, Nicholson DH. Subretinal

hemorrhage management by pars plana vitrectomy and internal drainage. Arch Ophthalmol. 1990;108:973-8.

9. Stifter E, Michels S, Prager F, Georgopoulos M, Polak K, Hirn C, et al. Intravitreal bevacizumab therapy for neovascular age-related macular degeneration with large submacular hemorrhage. Am J Ophthalmol. 2007;144:886-92.

10. Fine HF, Iranmanesh R, Del Priore LV, Barile GR, Chang LK, Chang S, et al. Surgical outcomes after massive subretinal hemorrhage secondary to age-related macular degeneration. Retina. 2010;30:1588-94.

11. Ohji M, Saito Y, Hayashi A, Lewis JM, Tano Y. Pneumatic displacement of subretinal hemorrhage without tissue plasminogen activator. Arch Ophthalmol. 1998;116:1326-32.

12. Kamei M, Tano Y, Maeno T, Ikuno Y, Mitsuda H, Yuasa T. Surgical removal of submacular hemorrhage using tissue plasminogen activator and perfluorocarbon liquid. Am J Ophthalmol. 1996;121:267-75.

13. Lim JI, Drews-Botsch C, Sternberg P Jr, Capone A Jr, Aaberg TM Sr. Submacular hemorrhage removal. Ophthalmology. 1995;102:1393-9.

14. Hassan AS, Johnson MW, Schneiderman TE, Regillo CD, Tornambe PE, Poliner LS, et al. Management of submacular hemorrhage with intravitreous tissue plasminogen activator injection and pneumatic displacement. Ophthalmology.

1999;106:1900-6.

15. Tsujikawa A, Sakamoto A, Ota M, Oh H, Miyamoto K, Kita M, et al. Retinal structural changes associated with retinal arterial macroaneurysm examined with optical coherence tomography. Retina. 2009;29:782-92.

16. Green WR, Key SN 3rd. Senile macular degeneration: a histopathologic study. Trans Am Ophthalmol Soc. 1977;75:180-254.

17. Reynders S, Lafaut BA, Aisenbrey S, Broecke CV, Lucke K, Walter P, et al. Clinicopathologic correlation in hemorrhagic age-related macular degeneration. Graefes Arch Clin Exp Ophthalmol. 2002;240:279-85.

18. Glatt H, Machemer R. Experimental subretinal hemorrhage in rabbits. Am J Ophthalmol. 1982;94:762-73.

19. Toth CA, Morse LS, Hjelmeland LM, Landers MB, 3rd. Fibrin directs early retinal damage after experimental subretinal hemorrhage. Arch Ophthalmol. 1991;109:723-9.

20. Koshibu A. [Ultrastructural studies on absorption of an experimentally produced subretinal hemorrhage. III. Absorption of erythrocyte break down products and retinal hemosiderosis at the late stage]. Nippon Ganka Gakkai Zasshi. 1979;83:386-400.

21. el Baba F, Jarrett WH 2nd, Harbin TS Jr, Fine SL, Michels RG, Schachat AP, et al.

Massive hemorrhage complicating age-related macular degeneration. Clinicopathologic correlation and role of anticoagulants. Ophthalmology. 1986;93:1581-92.

22. Drexler W, Sattmann H, Hermann B, Ko TH, Stur M, Unterhuber A, et al. Enhanced visualization of macular pathology with the use of ultrahigh-resolution optical coherence tomography. Arch Ophthalmol. 2003;121:695-706.

23. Ko TH, Fujimoto JG, Schuman JS, Paunescu LA, Kowalevicz AM, Hartl I, et al. Comparison of ultrahigh- and standard-resolution optical coherence tomography for imaging macular pathology. Ophthalmology. 2005;112:1922-35.

24. Wojtkowski M, Bajraszewski T, Gorczynska I, Targowski P, Kowalczyk A, Wasilewski W, et al. Ophthalmic imaging by spectral optical coherence tomography. Am J Ophthalmol. 2004;138:412-9.

25. Chen TC, Cense B, Pierce MC, Nassif N, Park BH, Yun SH, et al. Spectral domain optical coherence tomography: ultra-high speed, ultra-high resolution ophthalmic imaging. Arch Ophthalmol. 2005;123:1715-20.

26. Coscas F, Coscas G, Souied E, Tick S, Soubrane G. Optical coherence tomography identification of occult choroidal neovascularization in age-related macular degeneration. Am J Ophthalmol. 2007;144:592-9.

27. Coscas G, Coscas F, Vismara S, Zourdani A, Li Calzi CI. Clinical features and

natural history of AMD. In: Coscas G, Coscas F, Vismara S, Zourdani A, Li Calzi CI, editors. Optical coherance tomography in age-related macular degeneration. Heidelberg: Springer-Verlag, 2009:171-274.

28. Mavrofrides EC, Villate N, Rosenfeld PJ, Puliafito CA. Age-related macular degeneration, 2nd ed. In: Schuman JS, Puliafito CA, Fujimoto JG, editors. Optical coherence tomography. Thorofare: Slack, 2004:243-344.

29. Rosenfeld PJ, Brown DM, Heier JS, Boyer DS, Kaiser PK, Chung CY, et al. Ranibizumab for neovascular age-related macular degeneration. N Engl J Med. 2006;355:1419-31.

30. Spaide RF. Central serous chorioretinopathy. In: Holz FG, Spaide RF, editors. Medical retina. Berlin Heidelberg: Springer-Verlag 2004:77-93.

31. Lincoff H, Madjarov B, Lincoff N, Movshovich A, Saxena S, Coleman DJ, et al. Pathogenesis of the vitreous cloud emanating from subretinal hemorrhage. Arch Ophthalmol. 2003;121:91-6.

32. Ooto S, Tsujikawa A, Mori S, Tamura H, Yamashiro K, Otani A, et al. Retinal microstructural abnormalities in central serous chorioretinopathy and polypoidal choroidal vasculopathy. Retina. 2011;31:527-34.

33. Coscas G, Coscas F, Vismara S, Zourdani A, Li Calzi CI. OCT interpretation. In: Coscas G, Coscas F, Vismara S, Zourdani A, Li Calzi CI, editors. Optical coherance

tomography in age-related macular degeneration. Heidelberg: Springer-Verlag, 2009:97-170.

34. Marmor MF. Mechanisms of fluid accumulation in retinal edema. Doc Ophthalmol. 1999;97:239-49.

35. Costa RA, Calucci D, Skaf M, Cardillo JA, Castro JC, Melo LA Jr, et al. Optical coherence tomography 3: Automatic delineation of the outer neural retinal boundary and its influence on retinal thickness measurements. Invest Ophthalmol Vis Sci. 2004;45:2399-406.

36. Hayashi H, Yamashiro K, Tsujikawa A, Ota M, Otani A, Yoshimura N. Association between foveal photoreceptor integrity and visual outcome in neovascular age-related macular degeneration. Am J Ophthalmol. 2009;148:83-9.

37. Oishi A, Hata M, Shimozono M, Mandai M, Nishida A, Kurimoto Y. The significance of external limiting membrane status for visual acuity in age-related macular degeneration. Am J Ophthalmol. 2010;150:27-32.

38. Sandberg MA, Brockhurst RJ, Gaudio AR, Berson EL. The association between visual acuity and central retinal thickness in retinitis pigmentosa. Invest Ophthalmol Vis Sci. 2005;46:3349-54.

39. Bhisitkul RB, Winn BJ, Lee OT, Wong J, Pereira Dde S, Porco TC, et al. Neuroprotective effect of intravitreal triamcinolone acetonide against photoreceptor

apoptosis in a rabbit model of subretinal hemorrhage. Invest Ophthalmol Vis Sci. 2008;49:4071-7.

40. Kim KS, Lee WK. Bevacizumab for serous changes originating from a persistent branching vascular network following photodynamic therapy for polypoidal choroidal vasculopathy. Jpn J Ophthalmol. 2011;55:370-7.

41. Nakata I, Yamashiro K, Nakanishi H, Tsujikawa A, Otani A, Yoshimura N. VEGF gene polymorphism and response to intravitreal bevacizumab and triple therapy in age-related macular degeneration. Jpn J Ophthalmol. 2011;55:435-43.

42. Akaza E, Yuzawa M, Mori R. Three-year follow-up results of photodynamic therapy for polypoidal choroidal vasculopathy. Jpn J Ophthalmol. 2011;55:39-44.

43. Sho K, Takahashi K, Yamada H, Wada M, Nagai Y, Otsuji T, et al. Polypoidal choroidal vasculopathy: incidence, demographic features, and clinical characteristics. Arch Ophthalmol. 2003;121:1392-6.

Figure legends

Fig. 1 **a** A cross-sectional image of the fovea obtained with optical coherence tomography (OCT) of an eye with acute submacular hemorrhage associated with exudative age-related macular degeneration. Using an acute OCT image, three measurements were made in the fovea, including thickness of the neurosensory retina, thickness of the submacular hemorrhage, and total foveal thickness. **b** A cross-sectional image of the fovea obtained with OCT after resolution of the submacular hemorrhage. Using the final OCT image, three measurements were made in the fovea, including thickness of the neurosensory retina, thickness of the subretinal mass and Bruch's membrane, and total foveal thickness.

Fig. 2 Cross-sectional images obtained by optical coherence tomography (OCT) in eyes with acute submacular hemorrhage associated with exudative age-related macular degeneration. Each OCT section (middle in each case) was made along an arrow shown in the fundus photographs (left in each case). Magnified OCT images (right in each case) were made from the delimited boxes in OCT sections. **a** On the OCT section, submacular hemorrhage shows intensive hyperreflectivity beneath the neurosensory retina. Within the outer aspect of the neurosensory retina, several hyperreflective dots are seen. The structure of the neurosensory retina seems to be

relatively well preserved. Visual acuity was 0.5. **b** On the OCT section, submacular hemorrhage shows moderate hyperreflectivity. Amorphous hyperreflectivity and numerous hyperreflective dots are seen within the neurosensory retina. Visual acuity was 0.09. **c** On the OCT section, submacular hemorrhage shows moderate hyperreflectivity. Amorphous hyperreflectivity and numerous hyperreflective dots are seen in neurosensory retina, especially in the outer aspect. Under the fovea, infiltration of hemorrhage into the neurosensory retina seems to be blocked by the external limiting membrane (arrowheads). Visual acuity was 0.4. **d** On the OCT section, submacular hemorrhage shows intensive hyperreflectivity. Under the fovea, hemorrhage seems to invade the neurosensory retina beyond the external limiting membrane (arrowheads). Visual acuity was 0.08.

Fig. 3 Good recovery of vision in eyes with submacular hemorrhage associated with polypoidal choroidal vasculopathy. **a** A 66-year-old woman visited our clinic with a sudden decrease of vision in the right eye (0.2 OD), at which time she had a large submacular hemorrhage. **b** Initial horizontal (upper) and vertical (lower) optical coherence tomographic images along the white arrows shown in the fundus photograph show intensive hyperreflectivity of submacular hemorrhage beneath the neurosensory retina. Several hyperreflective dots are seen in the neurosensory retina; but structure

of the neurosensory retina seems to be well preserved. The line of the junction between inner and outer segments of the photoreceptors (IS/OS) is seen under the fovea. **c** At 12 months, submacular hemorrhage was completely absorbed. **d** Horizontal (upper) and vertical (lower) optical coherence tomographic images along the white arrows show good preservation of the neurosensory retina. The IS/OS line is seen under the fovea and visual acuity has improved to 0.8 in the right eye.

Fig. 4 Poor recovery of vision in eyes with submacular hemorrhage associated with polypoidal choroidal vasculopathy. **a** A 67-year-old man visited our clinic with a sudden decrease of vision in the left eye (0.4 OS), at which time he was noted to have a massive submacular hemorrhage. **b** Initial optical coherence tomographic image along the white arrow shown in the fundus photograph reveals intensive hyperreflectivity of the submacular hemorrhage beneath the neurosensory retina. Amorphous hyperreflectivity and hyperreflective dots are seen in overlying neurosensory retina. The line of the junction between inner and outer segments of the photoreceptors (IS/OS) is not detectable under the fovea. **c** At 14 months, the submacular hemorrhage has been absorbed completely. **d** Optical coherence tomographic image along the white arrow shows a thick subfoveal deposit. The IS/OS line is seen under the fovea, but visual acuity remained 0.3 in the left eye.

Table

Table 1 Initial and final conditions of patients with submacular hemorrhage associated with exudative age-related macular degeneration

Age (years)	76.8 ± 7.4
Gender (women/men)	10/21
Type of disease (typical AMD/PCV)	10/21
Initial examination	
Visual acuity (logMAR)	0.69 ± 0.45
Size of submacular hemorrhage (disc areas)	6.0 ± 3.1
Thickness of the neurosensory retina (μm)	194.3 ± 130.3
Thickness of the submacular hemorrhage (μm)	315.0 ± 222.5
Total foveal thickness (μm)	509.2 ± 281.0
Detection of IS/OS under the fovea (complete/incomplete/absent)	3/12/16
Detection of ELM under the fovea (complete/incomplete/absent)	21/2/8
Detection of RPE under the fovea (complete/incomplete/absent)	8/15/8
Duration of symptom (months)	3.7 ± 2.3
Follow-up (months)	11.3 ± 7.0
Final examination	
Visual acuity (logMAR)	0.69 ± 0.47
Cystoid macular edema (%)	11 (35.5%)
Subfoveal mass (%)	20 (64.5%)
Thickness of neurosensory retina (μm)	175.4 ± 136.3
Subretinal deposit and Bruch's membrane (μm)	169.5 ± 150.4
Total foveal thickness (μm)	363.7 ± 203.8
Detection of IS/OS under the fovea (complete/incomplete/absent)	3/8/20
Detection of ELM under the fovea (complete/incomplete/absent)	16/5/10

AMD, age-related macular degeneration; PCV, polypoidal choroidal vasculopathy; logMAR, logarithm of the minimum angle of resolution; IS/OS, junction between the inner and outer segments of the photoreceptors; ELM, external limiting membrane; RPE, retinal pigment epithelium.

Table 2 Association of initial visual acuity with other measurements obtained at the initial examination

	r	*p* value
Age (years)	0.018	0.922
Type of disease (typical AMD/PCV)	0.194	0.300
Size of submacular hemorrhage (disc areas)	0.411	0.022
Thickness of the neurosensory retina (μm)	0.203	0.274
Thickness of the submacular hemorrhage (μm)	0.485	0.0057
Total foveal thickness (μm)	0.478	0.0065
Detection of IS/OS under the fovea	0.272	0.139
Detection of ELM under the fovea	0.423	0.018
Detection of RPE under the fovea	0.479	0.0064

AMD, age-related macular degeneration; PCV, polypoidal choroidal vasculopathy; logMAR, logarithm of the minimum angle of resolution; IS/OS, junction between the inner and outer segments of the photoreceptors; ELM, external limiting membrane; RPE, retinal pigment epithelium.

Table 3 Association of final visual acuity with other measurements obtained at the final examination

	r	*p* value
Age (years)	0.244	0.186
Type of disease (typical AMD/PCV)	0.249	0.176
Duration of symptom (month)	0.182	0.327
Cystoid macular edema	0.355	0.050
Subfoveal mass	0.477	0.0067
Thickness of the neurosensory retina (μm)	0.277	0.132
Thickness of subretinal mass and Bruch's membrane (μm)	0.489	0.0052
Total foveal thickness (μm)	0.607	0.0003
Detection of IS/OS under the fovea (%)	0.574	0.0007
Detection of ELM under the fovea (%)	0.756	< 0.0001

AMD, age-related macular degeneration; PCV, polypoidal choroidal vasculopathy; LogMAR, logarithm of the minimum angle of resolution; RPE, retinal pigment epithelium; IS/OS, the junction between inner and outer segments of the photoreceptors; ELM, external limiting membrane.

Table 4 Association of final visual acuity with measurements obtained at the initial examination

	r	*p* value
Age (years)	0.244	0.186
Type of disease (typical AMD/PCV)	0.249	0.176
Size of subretinal hemorrhage (disc areas)	0.111	0.554
Visual acuity (logMAR)	0.295	0.107
Thickness of the neurosensory retina (μm)	0.100	0.594
Thickness of the submacular hemorrhage (μm)	0.268	0.145
Total foveal thickness (μm)	0.258	0.161
Detection of IS/OS under the fovea	0.375	0.038
Detection of ELM under the fovea	0.063	0.736
Detection of RPE under the fovea	0.281	0.126

AMD, age-related macular degeneration; PCV, polypoidal choroidal vasculopathy; logMAR, logarithm of the minimum angle of resolution; IS/OS, junction between the inner and outer segments of the photoreceptors; ELM, external limiting membrane; RPE, retinal pigment epithelium.

Figure 1
Click here to download high resolution image

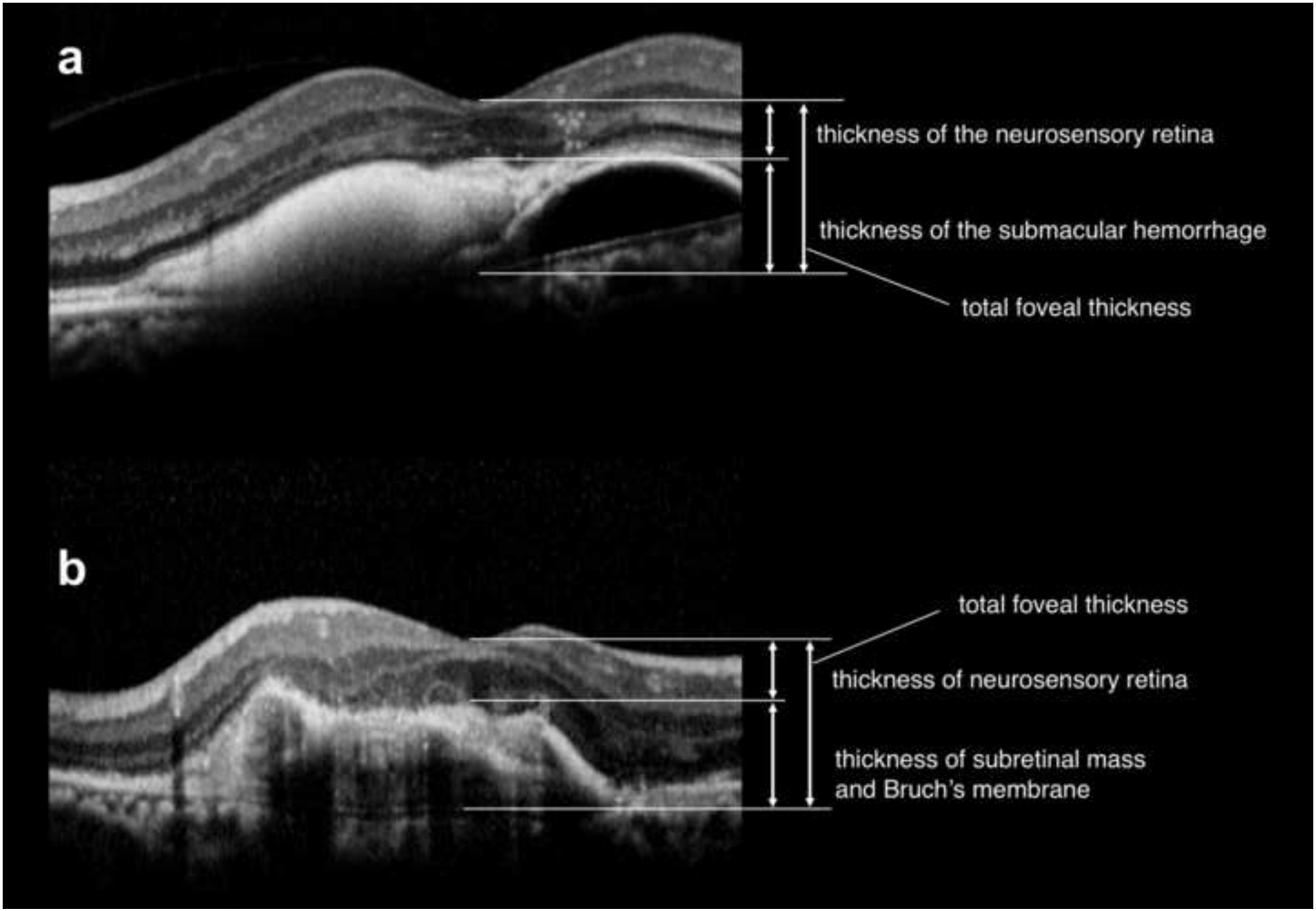

Figure 2
Click here to download high resolution image

Figure 3
Click here to download high resolution image

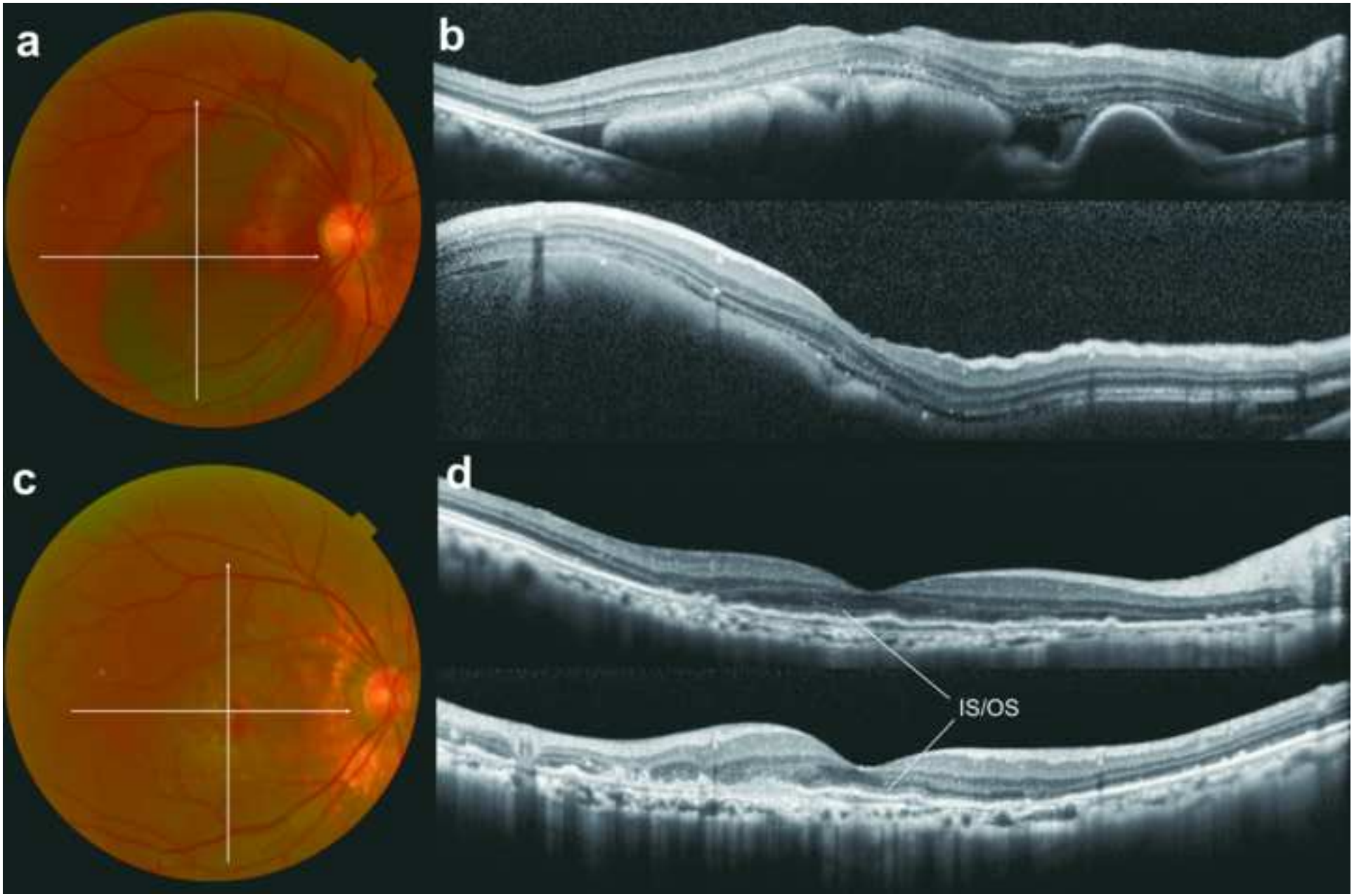

Figure 4
Click here to download high resolution image